Mon. Not. R. Astron. Soc. **297,** 427–434 (1998)

The *K*-band Hubble diagram for the brightest cluster galaxies: a test of hierarchical galaxy formation models

Alfonso Aragón-Salamanca,[1] Carlton M. Baugh[2] and Guinevere Kauffmann[3]

[1]*Institute of Astronomy, Madingley Road, Cambridge CB3 0HA*
[2]*Department of Physics, Science Laboratories, South Road, Durham DH1 3LE*
[3]*Max-Plank-Institut für Astrophysik, D-85740 Garching bei München, Germany*

Accepted 1998 January 29. Received 1998 January 29; in original form 1997 June 18

Downloaded from https://academic.oup.com/mnras/article/297/2/427/988365 by guest on 24 April 2024

ABSTRACT

We analyse the *K*-band Hubble diagram for a sample of brightest cluster galaxies (BCGs) in the redshift range $0 < z < 1$. In good agreement with earlier studies, we confirm that the scatter in the absolute magnitudes of the galaxies is small (0.3 mag). The BCGs exhibit very little luminosity evolution in this redshift range: if $q_0 = 0.0$, we detect *no* luminosity evolution; for $q_0 = 0.5$, we measure a small *negative* evolution (i.e., BCGs were about 0.5 mag fainter at $z = 1$ than today). If the mass in stars of these galaxies had remained constant over this period of time, substantial positive luminosity evolution would be expected: BCGs should have been *brighter* in the past, since their stars were younger. A likely explanation for the observed zero or negative evolution is that the stellar mass of the BCGs has been assembled over time through merging and accretion, as expected in hierarchical models of galaxy formation. The colour evolution of the BCGs is consistent with that of an old stellar population ($z_{\rm for} > 2$) that is evolving passively. We can thus use evolutionary population synthesis models to estimate the rate of growth in stellar mass for these systems. We find that the stellar mass in a typical BCG has grown by a factor $\simeq 2$ since $z \simeq 1$ if $q_0 = 0.0$, or by factor $\simeq 4$ if $q_0 = 0.5$. These results are in good agreement with the predictions of semi-analytic models of galaxy formation and evolution set in the context of a hierarchical scenario for structure formation. The models predict a scatter in the luminosities of the BCGs that is somewhat larger than the observed one, but that depends on the criterion used to select the model clusters.

Key words: galaxies: clusters: general – galaxies: elliptical and lenticular, cD – galaxies: evolution – galaxies: formation – infrared: galaxies.

1 INTRODUCTION

Brightest cluster galaxies (BCGs) have been extensively studied at optical wavelengths (Peach 1970, 1972; Gunn & Oke 1975, Sandage, Kristian & Westphal 1976; Kristian, Sandage & Westphal 1978; Hoessel 1980; Schneider, Gunn & Hoessel 1983a,b; Lauer & Postman 1992; Postman & Lauer 1995). The small scatter in their absolute magnitudes (< 0.3 mag up to $z \sim 0.5$; see, e.g., Sandage 1988) and their high luminosities make them useful standard candles for classical cosmological tests involving the Hubble diagram, such as the determination of q_0 and the variation of H_0 with redshift. However, there is now firm evidence that significant evolution has taken place in the colours and optical luminosities of early-type galaxies (including the BCGs) from $z \simeq 0$ to $z \simeq 1$ (e.g. Aragón-Salamanca et al. 1993; Rakos & Schombert 1995; Lubin 1996; Oke, Gunn & Hoessel 1996; Stanford, Eisenhardt & Dickinson, in preparation), implying that the Hubble diagram could be seriously affected by evolutionary changes even at relatively modest redshifts. Conclusions concerning q_0 cannot be derived from such diagrams until these changes are well understood. Indeed, the Hubble diagram for the BCGs may well have more to teach us about galaxy evolution than about cosmology.

The study of the BCGs in the near-infrared *K* band (2.2 μm) has two main advantages over optical studies: first, the *k*-corrections are appreciably smaller (indeed, they

© 1998 RAS

are negative) and virtually independent of the spectral type of the galaxies (see, e.g., Aragón-Salamanca et al. 1993, 1994) and, second, the light at long wavelengths is dominated by long-lived stars. Thus the *K*-band luminosity is a good measure of the total stellar mass in the galaxies.

The *K*-band Hubble diagram has long been used as an evolutionary diagnostic for radio galaxies (Grasdalen 1980; Lebofsky 1980; Lilly & Longair 1982, 1984; Lebofsky & Eisenhardt 1986; Lilly 1989,ab), which also have a relatively small intrinsic dispersion in their luminosities ($\simeq 0.4$ mag for $1 < z < 2.2$; Lilly 1989a). Substantial positive luminosity evolution was found: radio galaxies were about 1 mag brighter at $z \simeq 1$ than they are today. Aragón-Salamanca et al. (1993) measured *K*-band luminosities for a sample of 19 BCGs in the redshift range $0 < z < 1$ and found that the *K* magnitude–redshift relation is tighter (scatter = 0.3 mag) than for radio galaxies. Moreover, these authors did not detect significant *K* luminosity evolution for the BCGs, and concluded that their evolutionary properties were different from those of radio galaxies: powerful radio galaxies are apparently less homogeneous in their evolutionary behaviour and show stronger luminosity evolution. Aragón-Salamanca et al. also found that the colours of the early-type galaxies (including the BCGs) in these clusters have evolved since $z \simeq 1$ at a rate consistent with a scenario in which the bulk of their stars formed at relatively high redshifts ($z > 2$) and evolved passively thereafter. This conclusion has been confirmed by several more recent studies (Rakos & Schombert 1995; Lubin 1996; Oke et al. 1996; Ellis et al. 1997; Stanford, Eisenhardt & Dickinson, in preparation).

The recent development of *semi-analytic techniques* has provided theorists with the tools to make predictions for the formation and evolution of galaxies, using physically motivated models set in the context of hierarchical structure formation in the Universe (e.g. Cole 1991; Lacey & SIlk 1991; White & Frenk 1991; Kauffmann, White & Guiderdoni 1993; Cole et al. 1994; Kauffmann, Guiderdoni & White 1994; Heyl et al. 1995). The properties of galaxies in these models are in broad agreement with the present-day characteristics of galaxies, such as the distribution of luminosities, colours and morphologies, and with the properties of galaxies at high redshift, including the faint galaxy counts, colours and redshift distributions (e.g. Kauffmann 1995, 1996; Baugh, Cole & Frenk 1996a; Baugh et al. 1998; Kauffmann & Charlot 1998). In this paper, we will test whether the models also predict the right behaviour for a special class of galaxies, namely the BCGs. In the models, these galaxies grow in mass both from the cooling of gas from the surrounding hot halo medium and from the accretion of 'satellite' galaxies that fall to the cluster centre as result of dynamical friction and then merge.

In Section 2 we present the observational results and derive the luminosity evolution of the BCGs in the sample. In Section 3 we briefly describe two independent semi-analytic models of galaxy formation, outline their basic assumptions, limitations and uncertainties, and discuss the predictions they make for the evolution of the BCGs. Section 4 compares the model predictions with the observational results.

2 OBSERVATIONAL RESULTS

2.1 Photometric data

The clusters in our sample are all optically selected, although most of them have also been detected in X-rays. At $z \leq 0.37$ they come from the Abell (1957) and Abell, Corwin & Olowin (1989) catalogues. At higher redshifts they have been found from the projected density contrast in deep optical imaging surveys (Gunn, Hoessel & Oke 1986; Couch et al. 1991), and should represent the richest clusters present at each redshift.

The *K*-band data analysed here come from the photometric study carried out by Aragón-Salamanca et al. (1993) of galaxy clusters in the $0 < z < 1$ redshift range (19 BCGs), complemented with new *K*-band images of three clusters at $z \simeq 0.3$ (Barger et al. 1996) and six clusters with $0.39 \leq z \leq 0.56$ (Barger et al. 1998). The images were obtained at the 3.8-m UK Infrared Telescope (UKIRT), the 3.9-m Anglo-Australian Telescope (AAT) and the 1.52-m Palomar Observatory Telscope (POT). There is some overlap in the clusters observed by Aragón-Salamanca et al. and Barger et al., bringing the number of BCGs studied here to a total of 25 (see Table 1). For the clusers in common, both sets of photometry agree very well (within the estimated errors), and we have chosen the better quality image in each case.

We refer the reader to the original papers for a detailed description of the data. We will concentrate here on the aspects relevant to this paper. The photometric zero-point uncertainties in the *K*-band images were always small (0.02–0.04 mag) and are completely negligible for our analysis. As in Aragón-Salamanca et al. (1993), *K*-band photometry for the BCGs was obtained inside a fixed metric aperture of 50-kpc diameter,[1] so that the minimum aperture at high redshift is ~ 5 arcsec, thus minimizing the effect of seeing. Because of the ambiguity of what constitutes a 'galaxy' (~ 30 per cent of local first-ranked cluster galaxies are multiple-nucleus systems: i.e., more than one 'galaxy' occurs within our metric aperture – see Hoessel 1980) we follow the approach of Schneider et al. (1983a) and adopt a working definition of the brightest cluster galaxy as *the region of maximum cluster light enclosed in our metric aperture.* The photometry data from the AAT and POT was transformed into the *K*-band system of the UKIRT (where most of the data come from) using colour terms determined from the known filter responses. The colour terms were always ≤ 0.08 mag, and we estimate that the uncertainty in the transformation is well below 2 per cent and thus negligible. Galactic reddening corrections were estimated from Burstien & Heiles' (1982) maps, but since the galactic latitudes were always reasonably high, they were very small in the *K*-band. Finally, small seeing corrections and *k*-corrections wre also applied, as in Aragón-Salamanca et al. Table 1 contains the corrected *K* magnitudes for the BCG sample. Values for $q_0 = 0.0$ and 0.5 are given to account for the difference in projected aperture at a given metric aper-

[1] $H_0 = 50$ km s^{-1} Mpc^{-1} assumed throughout. Because of the uncertainty in the value of q_0 we will carry out parallel analysis for $q_0 = 0.0$ and 0.5.

Downloaded from https://academic.oup.com/mnras/article/297/2/427/988365 by guest on 24 April 2024

Table 1. Corrected rest frame *K*-band magnitudes for the BCGs.

Cluster	z	$K^0_{q0=0.0}$	$K^0_{q0=0.5}$	reference
Abell 1656[a](NGC4889)	0.023	8.89	8.88	(1)
Abell 2199 (NGC6166)	0.030	9.50	9.49	(1)
Abell 2197 (NGC6173)	0.031	9.54	9.53	(1)
Abell 2151 (NGC6034)	0.037	10.49	10.38	(1)
Abell 963	0.206	13.61	13.55	(1)
Abell 1942	0.224	13.92	13.88	(1)
AC103	0.310	14.62	14.56	(2)
AC114	0.310	14.54	14.46	(2)
AC118	0.310	14.77	14.67	(2)
Cl2244−02	0.329	15.35	15.31	(1)
Abell 370	0.374	15.05	14.95	(1)
Cl0024+16	0.391	15.29	15.14	(1),(3)
3C295	0.460	15.26	15.14	(3)
Cl0412−65[b]	0.510	15.60	15.55	(3)
Cl1601+42	0.540	16.23	16.13	(3)
Cl0016+16	0.546	16.21	16.02	(1),(3)
Cl0054−27[c]	0.563	16.50	16.37	(1),(3)
Cl0317+1521	0.583	17.08	17.01	(1)
Cl0844+18[d]	0.664	16.93	16.80	(1)
Cl1322+3029	0.697	16.90	16.72	(1)
Cl0020+0407	0.698	17.06	17.01	(1)
Cl1322+3027	0.751	16.97	16.79	(1)
Cl2155+0334	0.820	17.22	17.12	(1)
Cl1603+4313	0.895	17.78	17.64	(1)
Cl1603+4329	0.920	18.24	18.02	(1)

[a]Coma cluster.
[b]Also known as F1557.19TC (Couch et al. 1991).
[c]Also known as J1888.16CL (Couch et al. 1991).
[d]Also known as F1767.10TC (Couch et al. 1991).
References. (1) Aragón-Salamanca et al. 1993; (2) Barger et al. 1996; (3) Barger et al. 1998.

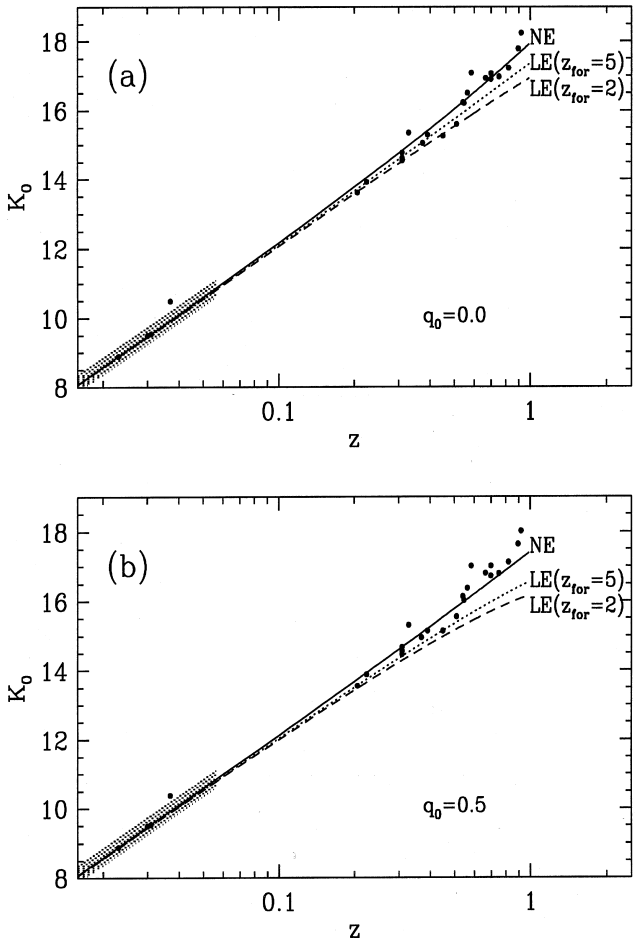

Figure 1. (a) Magnitude–redshift relation (Hubble diagram) for the brightest cluster galaxies in the rest frame *K*-band. The *K* magnitudes have been measured inside a projected 50-kpc-diameter aperture. The solid line shows the no-evolution prediction, normalized to the low-redshift data. The dashed line corresponds to the luminosity evolution expected for a stellar population formed at $z_{for}=2$ evolving passively. The dotted line shows the evolution expected for $z_{for}=5$. The shaded area at low-redshift represents the *K*-band magnitudes of $z<0.06$ BCGs estimated from the *R*-band data of Postman & Lauer (1995). The width of the shaded area reflects the observed scatter (see text for details). $H_0=50$ km s^{-1} Mpc^{-1} and $q_0=0.0$ were assumed. (b) As (a), but for $q_0=0.5$.

ture as a function of the deceleration parameter. We estimate that the total uncertainty of the corrected magnitudes is below 10 per cent, and will contribute very little to the observed scatter (see original data papers for a detailed discussion of the uncertainties).

Fig. 1 shows the *K* magnitude–redshift relation (Hubble diagram) for the BCGs in our sample. The solid lines show no-evolution predictions which only take into account the distance modulus as a function of *z*, normalized to the three lowest redshift points. Since we do not have *K* magnitudes for many low-redshift galaxies, the normalization of the no-evolution line could be somewhat uncertain. However, extensive optical photometry exists and, given the homogeneity in the colours of these galaxies (Postman & Lauer 1995), we feel justified to use the *R*-band photometry of Lauer & Postman (1992) to estimate *K*-band magnitudes. The shaded area at low-redshift in Fig. 1 represents the *K*-band magnitudes for $z<0.06$ BCGs estimated from the *R*-band data of Postman & Lauer, corrected to our metric aperture (using d log L/d log $r=0.5$, from the same authors), and assuming a typical $R-K=2.6$ (cf. Bower, Lucey & Ellis 1992a,b). The width of the shaded area reflects the observed scatter. The agreement with our local normalization is remarkably good.

In agreement with the results of Aragón-Salamanca et al., the scatter of the observed magnitudes around the no-evolution prediction is 0.30 mag. Assuming that the *K*-band light provides an estimate of the total stellar mass of the galaxies, this very low scatter implies that BCGs at a given redshift have very similar masses in stars (within 30 per cent rms), which has yet to be explained by any model of galaxy formation (see Section 3).

Morphological information is available for the low-redshift clusters from the ground-based images. Many of intermediate- and high-redshift clusters have been imaged with *HST*; thus morphological information exists for 16 of the $z>0.3$ clusters (Smail et al. 1996, 1997; Couch et al., in preparation). In general, the BCGs are either cD galaxies or giant ellipticals, although for the highest-*z* clusters there could be some ambiguity since the extended cD haloes might not be clearly visible, given the relatively high surface

Downloaded from https://academic.oup.com/mnras/article/297/2/427/988365 by guest on 24 April 2024

brightness limits achievable with *HST*. Thus some of the BCGs classified as ellipticals could be cD galaxies. The exception to this rule is the BCG in the 3C 295 cluster, which is a radio galaxy and shows an unresolved AGN-like morphology in a disturbed disc or envelope.

The optical and optical–infrared colours (from ground-based and *HST* data) of the BCGs are compatible with those of the colour–magnitude sequence of cluster elliptical and S0 galaxies. The exception is, again, 3C 295, which is substantially bluer (by $\simeq 0.8$ mag in $R-K$). The peculiar colours and morphology of this galaxy are probably related to its being a powerful radio source. However, its *K*-band luminosity agrees very well with that of the rest of the BCGs in our sample, and we have kept it in our analysis. Taking it out would not alter our conclusions.

2.2 Interpretation using evolutionary synthesis models

Fig. 1 shows that the luminosity of the BCGs (inside a fixed metric aperture of 50-kpc diameter) does not evolve strongly with redshift. This is shown more clearly in the top panel of Fig. 2, where the no-evolution prediction has been subtracted from the data. It is clear that for $q_0=0.0$ the observed magnitudes do not seem to evolve with redshift. For $q_0=0.5$ there is a hint of *negative* evolution: BCGs at high redshift tend to be marginally fainter than low-redshift ones.

A convenient parametrization of the luminosity evolution is $L_K(z)=L_K(0)\times(1+z)^{\gamma}$. Least-squares fits to the data yield $\gamma=-0.06\pm0.3$ and -0.6 ± 0.3 for $q_0=0.0$ and 0.5 respectively. Thus the BCGs show *no* or *marginally negative* luminosity evolution. However, as mentioned above, the colours of these galaxies show the same evolution as the early-type cluster galaxies: they become progressively bluer with redshift at a rate which indicates that their stellar populations were formed at $z>2$ and evolved passively thereafter. If the total stellar mass of the galaxies has remained constant, we would expect them to become progressively *brighter* with redshift, as the average ages of their stellar populations become younger. Since that brightening is not observed, the most likely explanation is that the total mass in stars in the BCGs has not remained constant, but has grown with time. We will now estimate the rate of this growth.

We used evolutionary population synthesis models (Bruzual & Charlot, in preparation; see also Bruzual & Charlot 1993) to predict the expected luminosity evolution of a passively evolving stellar population formed at a given redshift. That should represent the brightening of the stellar populations due to the decrease in average stellar age with redshift. A Scalo (1986) initial mass function with stellar masses in the range $0.1\leq m\leq 125\ \mathrm{M}_{\odot}$ was assumed. The exact value of the upper mass limit is not critical, given the expected ages of the stellar populations in the observed redshift range, provided that it is above the turn-off mass at the ages corresponding to $z<1$. The model predictions are plotted in Fig. 1 (LE lines) for formation redshifts $z_{\rm for}=2$ and 5. These models produce a colour evolution compatible with the observations of early-type cluster galaxies. Note that $z_{\rm for}<2$ is clearly ruled out by the observed *slow* colour evolution (cf. Section 1). Making $z_{\rm for}>5$ makes very little difference to the age of the stars. We have assumed solar metallicity, but changing the metal content does not significantly alter the predictions. Other models (e.g. Arimoto & Yoshii 1986; Kodama & Arimoto 1997) predict very similar luminosity evolution; thus we believe that the models considered here bracket reasonably well the luminosity evolution expected from the colour constraints, and that the predictions are not very model-dependent.

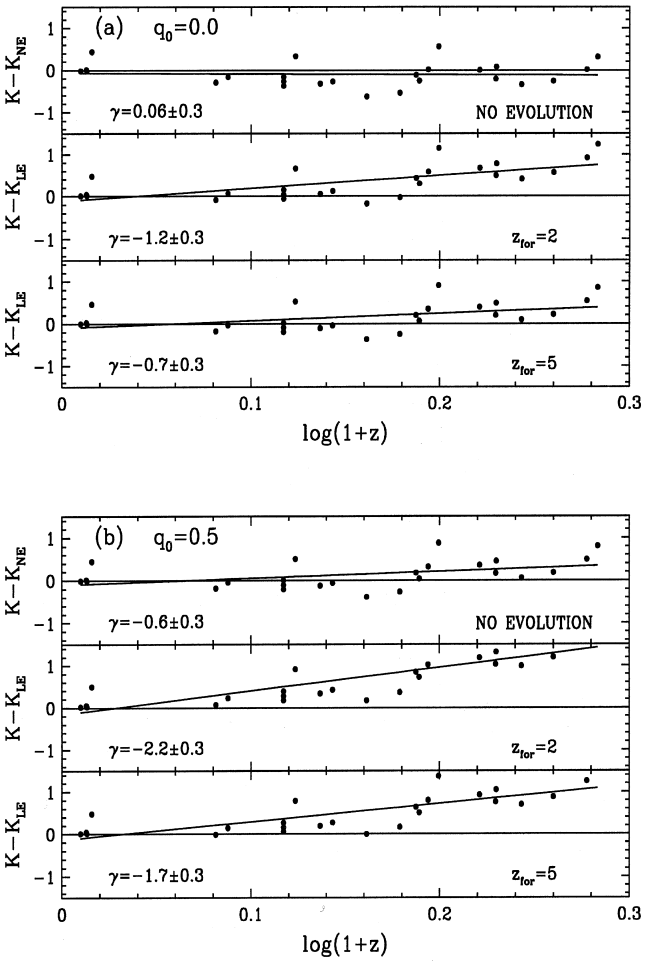

Figure 2. (a) Top panel: the same data presented in Fig. 1 after subtracting the no-evolution prediction. Middle and bottom panels: the same data after subtracting models for luminosity evolution in which the BCG stars form at $z_{\rm for}=2$ and 5 respectively and evolve passively thereafter (for $q_0=0.0$). The solid lines represent least-squares linear fits. (b) As (a), but for $q_0=0.5$.

In Fig. 2 (lower two panels) we have plotted the observed magnitudes after subtracting the luminosity evolution predictions. Since the models assume a constant stellar mass, the rate of change with redshift in the *K* magnitudes, after correcting for the expected brightening due to passive evolution, should be a direct measurement of the rate of change in stellar mass. Note that, strictly speaking, what we call 'mass in stars' really means 'mass in luminous stars', i.e., those which contribute to the galaxy *K*-band light. Parametrizing the evolution as $M_*(z)=M_*(0)\times(1+z)^{\gamma}$, least-squares fits give the following results:

$q_0=0.0$ $\quad z_{\rm for}=2 \quad \gamma=-1.2\pm0.3$

$\quad\quad\quad z_{\rm for}=5 \quad \gamma=-0.7\pm0.3$

Downloaded from https://academic.oup.com/mnras/article/297/2/427/988365 by guest on 24 April 2024

$q_0 = 0.5 \qquad z_{\rm for} = 2 \qquad \gamma = -2.2 \pm 0.3$

$\qquad\qquad z_{\rm for} = 5 \qquad \gamma = -1.7 \pm 0.3.$

These rates imply that the mass in stars of a typical BCG grew by a factor $\simeq 2$ if $q_0 = 0.0$, or $\simeq 4$ if $q_0 = 0.5$, from $z \simeq 1$ to $z \simeq 0$, i.e., in the last $\simeq 8$–10 Gyr.

At this point we would like to make a historical comment. One of us (AAS) carried out the analysis described in this section *independently* of the rest of the authors and invited the Durham and Munich groups to make predictions, using the semi-analytic models described in Section 3, for the growth of the stellar mass in BCGs as a function of redshift. In the first instance, this was done *without any prior knowledge of the observationally determined rates* and without any interaction between the two groups to ensure that the predictions where truly independent. The surprising level of agreement of the model predictions with each other, and with the observations, encouraged us to compare the model output with the data in more detail. This is presented in the next section.

3 GALAXY FORMATION AND EVOLUTION MODELS

In his section, we discuss the predictions of the semi-analytic models of the Durham and Munch groups. Full details of the Durham models can be found in Cole et al. (1994) and Baugh, Cole & Frenk (1996b). The version of the Munich models used here is the same as that described in Kauffmann & Charlot (1998). Further details about the Munich models can be found in Kauffmann et al. (1993). Although the two models are very similar in outline and in their basic framework, many features, e.g., the simple parameterizations used to describe star formation and feedback, are different in detail.

Briefly, the hierarchical collapse and merging of an ensemble of dark matter haloes is followed using Monte Carlo techniques. Gas virializes in the dark matter haloes, cools radiatively and condenses on to a *central* galaxy at the core of each halo. Star formation occurs at a rate proportional to the mass of cold gas present. The supply of cold gas is regulated by feedback processes associated with star formation, such as stellar winds and supernovae. As time proceeds, a halo will merge with a number of others, forming a new halo of larger mass. All gas which has not already cooled is assumed to be shock-heated to the virial temperature of this new halo. This hot gas then cools on to the central galaxy of the new halo, which is identified with the central galaxy of its *largest progenitor.* The central galaxies of the other progenitors become *satellite galaxies*, which are able to merge with the central galaxy on a dynamical friction time-scale. If a merger takes place between two galaxies of roughly comparable mass, the merger remnant is labelled as an 'elliptical' and all cold gas is transformed instantaneously into stars in a 'starburst'. The same stellar population models (Bruzual & Charlot, in preparation) used in Section 2.2 are employed to turn the star formation histories of the model galaxies into broad-band luminosities.

In these models, there are three different ways in which the stellar masses of the brightest galaxies in clusters can grow:

(i) merging of satellite galaxies that sink to the centre of the halo through dynamical friction;

(ii) quiescent star formation as a result of gas cooling from the surrounding hot halo medium, and

(iii) 'bursts' of star formation associated with the accretion of a massive satellite.

As noted by Kauffmann et al. (1993), the colours and absolute magnitudes of central cluster galaxies are predicted to be bluer and brighter than observed if all the gas present in the cooling flows of massive clusters turns into visible stars. To overcome this problem, these authors simply switched off star formation in cooling flows when the circular velocity of the halo exceeded 500 km s^{-1}. This value was chosen so as to obtan a good fit to the bright end of the Virgo cluster luminosity function. Another solution is to assume that gas in the central regions of haloes follows a different density profile from that of the dark matter. In particular, if the gas has a constant density core, cooling is very much less efficient in the centres of massive clusters. The precise form of the gas density profile is much less important for cooling in low-mass haloes, since these objects are denser and have much shorter cooling times.

In Fig. 3, we consider the evolution of a subset of the $z = 0$ BCGs in a model with star formation switched off in haloes with circular velocity greater than 500 km s^{-1}. The solid line shows the cumulative growth in stellar mass of the BCG due to merging events. The dashed line shows the cumulative contribution from stars formed from quiescently cooling

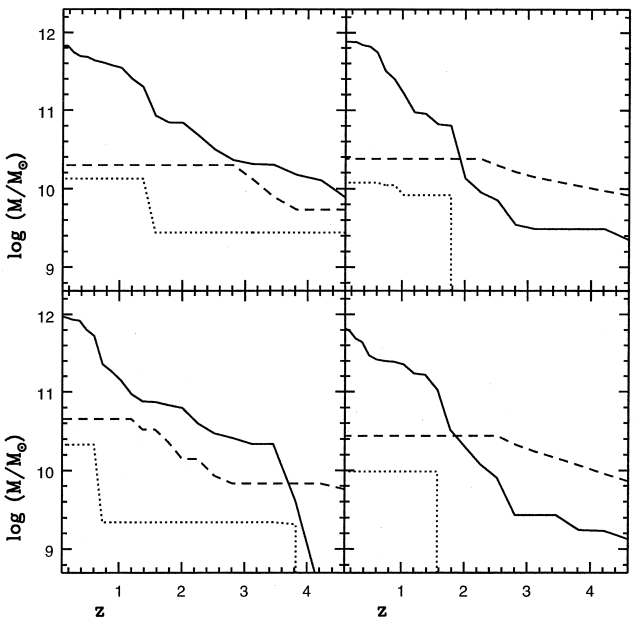

Figure 3. The build-up in stellar mass of the largest progenitor in four examples of BCGs taken from the Munich models, which reside in dark matter haloes with circular velocity 1000 km s^{-1} at the present time. Star formation is switched off in any progenitor halo whose circular velocity is in excess of 500 km s^{-1}. The solid lines show the accumulation of stellar mass from merging events, the dashed lines show the mass contributed by stars forming from gas cooling from the surrounding hot halo medium, and the dotted lines show the mass contributed by star formation bursts associated with major mergers.

Downloaded from https://academic.oup.com/mnras/article/297/2/427/988365 by guest on 24 April 2024

gas, and the dotted line is the contribution from stars formed in bursts during major mergers. As can be seen, star formation from bursts and cooling gas account for only a few per cent of the final mass of the BCG. The rest comes from accreted galaxies. The four panels in the figure represent independent Monte Carlo realizations of the formation of a BCG in a halo of circular velocity 1000 km s^{-1}. It is striking that although each BCG gas a significantly different merging history, their final stellar masses differ very little from one realization to another.

We will now make a comparison with the data presented in Section 2. The observational selection picks out *the richest clusters* at each redshift, but the sample is not complete in any well-defined sense. We mimic the observational selection as best we can by calculating the masses of BCGs in haloes with circular velocities greater than some fixed value as a function of redshift. This means we are selecting rarer objects with increasing redshift. We also explore the effect of selecting clusters by mass instead of circular velocity.

We present the model predictions for two cold dark matter (CDM) cosmologies, namely one with the critical density, and an open model with density parameter $\Omega_0 = 0.2$. The density fluctuations in each case are normalized to reproduce the abundance of rich clusters (e.g. White, Efstathiou & Frenk 1993; Eke, Cole & Frenk 1996; Viana & Liddle 1996). At several redshifts in the range $0 \leq z \leq 1$, we have selected ~ 200 haloes with circular velocities greater than 700 km s^{-1}. Note that the clusters are weighted so that they are representative of the mass distribution of haloes at the given redshift.

The evolution of the average stellar mass of the brightest galaxies in the haloes with redshift is shown in Fig. 4. We have divided the average mass of the BCGs at each redshift by the average mass of BCGs found in the redshift-zero clusters. The open triangles show the results of the Durham models, which adopt the halo density profile of Navarro, Frenk & White (1996) for the dark matter. The gas is assumed to follow a different density profile, with a constant density at the core of the halo (full details of these extensions to the original Cole et al. 1994 model will be given in Cole et al., in preparation). The filled circles show the predictions of the Munich models, in which isothermal density profiles are assumed for both the gas and the dark matter. Star formation is switched off in haloes with a circular velocity in excess of 500 km s^{-1}. The curves show the growth in stellar mass with redshift of the BCGs deduced in Section 2.2; the dotted lines show the parametrization with $z_{for} = 5$, whilst the dashed line shows $z_{for} = 2$. Both models fit the observed evolution very well.

In Fig. 5, we show the evolution in the average rest frame $V-I$ colours of the BCGs. Once again, the open triangles show the Durham models, and the filled circles the Munich models. The curves are a fit to the observed colour evolution given in Aragón-Salamanca et al. (1993). For the $\Omega = 1$ cosmology, both models fit the observed colour evolution reasonably well. The Durham models predict larger scatter

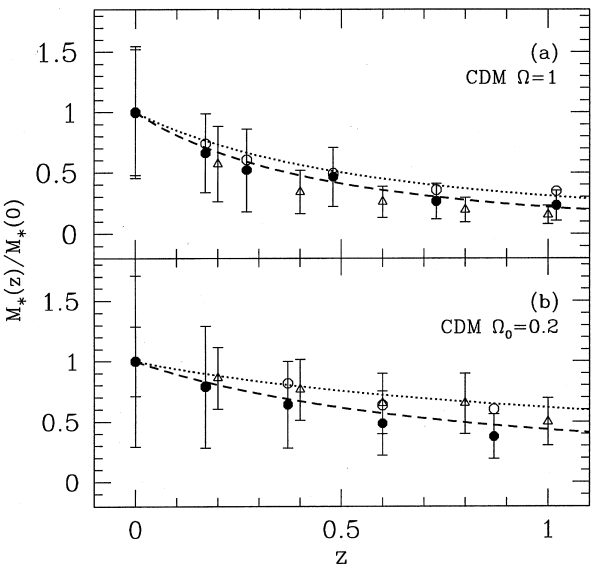

Figure 4. The average stellar mass of BCGs as a function of redshift. We have selected galaxies at each epoch that reside in haloes with circular velocities greater than 700 km s^{-1}. The points have been normalized by dividing by the average stellar mass of the BCGs in each model at $z = 0$. (a) shows the predictions for a cold dark matter universe with the critical density, whilst (b) shows an open universe with a present-day density parameter of $\Omega_0 = 0.2$. In each panel, the filled circles show the results from the Munich models, and the open triangles show the results of the Durham models. The curves show the trends in stellar mass deduced in Section 2.2; the dotted curve corresponds to $z_{for} = 5$, and the dashed curve to $z_{for} = 2$. The open circles in (a) and (b) show the evolution in the average stellar mass of the BCGs predicted by the Munich model when a cut in halo mass of $2 \times 10^{14}\ h^{-1}\ M_{\odot}$ is applied to select clusters at each redshift.

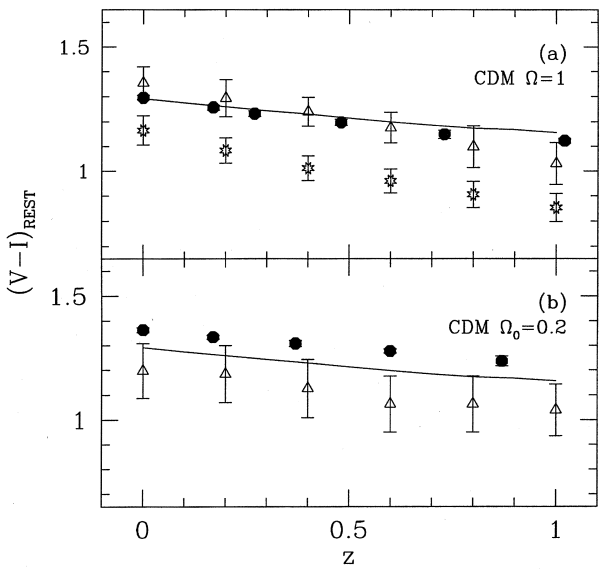

Figure 5. The rest frame $V-I$ colour of the model BCGs as a function of redshift. Again, (a) shows the results for a critical-densith CDM universe, whilst (b) shows the model output for an open universe with $\Omega = 0.2$. The filled symbols show the Munich models, and the open symbols show the Durham models. The open stars in (a) show a Durham model in which the gas density profile is the same as that of the dark matter in the halo. Hence gas cools more efficiently and more recent star formation takes place, making the BCGs bluer. The line is a fit to the observed colour evolution of the BCGs taken from Aragón-Salamanca et al. (1993).

Downloaded from https://academic.oup.com/mnras/article/297/2/427/988365 by guest on 24 April 2024

in the colours, because the BCGs are still undergoing some low-level star formation, whereas the BCGs in the Munich models have ceased forming stars altogether. For reference, we also show a model (shown by the open stars) where cooling and star formation are efficient at the centres of massive clusters. This is a model where both the gas and the dark matter follow the standard Navarro, Frenk & White (1996) density profile. In this case, the colours are too blue by $\sim$0.1–0.2 mag. In the low-density cosmology, it is interesting that the Durham and Munich models exhibit *opposite* trends in colour. The Munich models are redder than in a flat cosomology, because the BCGs form earlier and contain older stars. On the other hand, the Durham models are bluer. This is because haloes in a low-density universe are more concentrated and gas still cools at the cluster centres, even if a different density profile is assumed.

An important question to consider is how our results would be affected by adopting a different selection criterion for the clusters in the model. To explore this, Fig. 6(a) shows how the average mass of a $z=0$ BCG changes as a function of circular velocity cut-off for both the Munich and Durham models. This plot shows that more massive BCGs are found in more massive haloes. The stellar mass of a BCG changes by a factor of 2 for a factor of 5 increase in halo mass. Fig. 6(b) shows how the predicted scatter in *K*-band absolute magnitude changes as a function of circular velocity cut-off. As can be seen, the scatter decreases as richer clusters are selected. Both the Munich and Durham models predict larger scatter than that observed, although the discrepancy is worse for the Durham models.

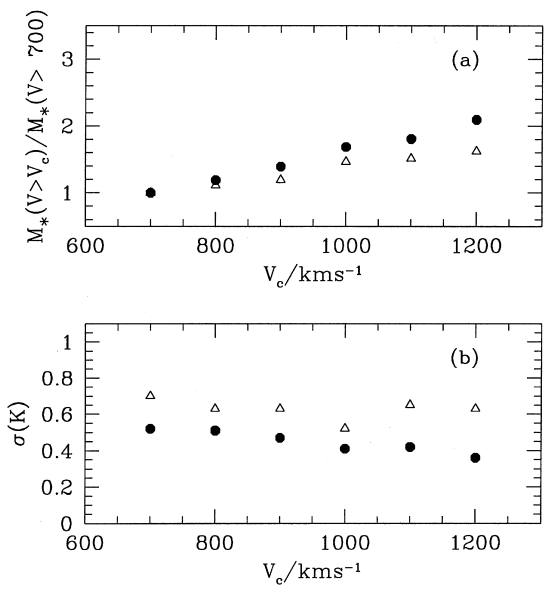

Figure 6. (a) The average stellar mass of BCGs at $z=0$ as a function of the circular velocity cut used to select clusters. The mean BCG mass increases by a factor of 2 over a range in circular velocity that corresponds to an increase by a factor of 5 in dark matter halo mass. The filled symbols show the Munich results, and the open symbols show the Durham results. (b) The scatter in the absolute *K* magnitudes of BCGs as a function of the circular velocity used to define the cluster sample. The Durham models predict a larger scatter than the Munich models.

It should be noted that clusters of fixed circular velocity are less massive at high redshift by a factor $\simeq(1+z)^{3/2}$ (this scaling arises from the fact that haloes collapse and virialize at a density $\sim 200\bar{\rho}(z)$, where $\bar{\rho}(z)$ is the mean density of the Universe at redshift z). Selecting clusters according to a halo mass cut-off, rather than a circular velocity cut-off, will thus select more massive BCGs at high redshift. The effect of mass selection on the predicted evolution is shown by the open circles in Fig. 4, where we have selected clusters greater than 2×10^{14} $M_\odot$ at each redshift. The mass evolution is now slightly weaker, but the effect is small and the model results are still in good agreement with the observations.

4 DISCUSSION

We have shown that the *K*-band Hubble diagram for a sample of brightest cluster galaxies in the redshift range $0<z<1$ has a very small scatter (0.3 mag), in good agreement with earlier studies. The BCGs exhibit very little luminosity evolution in this redshift range: if $q_0=0.0$, we detect *no* luminosity evolution; for $q_0=0.5$, we measure a small *negative* evolution (i.e., BCGs were about 0.5 mag fainter at $z=1$ than today). However, substantial *positive* luminosity evolution would be expected if the mass in stars of these galaxies had remained constant over this period of time: BCGs should have been *brighter* in the past, since their stars were younger. The most likely explanation for the observed zero or negative evolution is that the stellar mass of the BCGs has been assembled over time through merging and accretion, as expected in hierarchical models of galaxy formation. Since the colour evolution of the BCGs is consistent with that of an old stellar population ($z_{for}>2$) that is evolving passively, we have used evolutionary population synthesis models to estimate the rate of growth in stellar mass for these systems. We find that the stellar mass in a typical BCG has grown by a factor of $\simeq2$ since $z\simeq1$ if $q_0=0.0$, or by factor of $\simeq4$ if $q_0=0.5$.

Two independent groups of galaxy formation modellers predicted the decrease in stellar mass of the BCGs with increasing redshift, in advance of seeing the data and without any fine-turning of their semi-analyic model parameters. We have extracted the properties of BCGs in massive haloes with circular velocities greater than 700 km s^{-1} or masses greater than 2×10^{14} $M_\odot$, at various redshifts. The average stellar mass of the BCGs increases by a factor of $\sim$4–5 in the critrical-density models. In the low-density models, the growth in stellar mass is more modest, i.e., a factor of 2–3. This is because clusters assmeble at higher redshift in a low-density universe. Note, however, that both models agree well with the data when the appropriate value of q_0 is used in the analysis. It is not possible to make statements about a preferred cosmology from this exercise.

We also find that in order to reproduce the observed colours of the galaxies, some mechanism must act to suppress visible star formation in the cooling flows of the most massive haloes. It has been postulated that much of this gas may be forming low-mass stars (Fabian, Nulsen & Canizares 1982) or cold gas clouds (White et al. 1991). Another possibility we have explored is that the gas may be less concentrated in the centres of clusters than the dark matter, and hence not able to cool efficiently. In both cases, the

Downloaded from https://academic.oup.com/mnras/article/297/2/427/988365 by guest on 24 April 2024

evolution in the *K*-band luminosities of the BCGs comes about almost exclusively as a result of the merging of satellite galaxies in the cluster. An important and unanticipated result of our analysis is that the predicted scatter in the stellar masses of the BCGs built through merging and accretion is still quite small, though somewhat larger than the observed one. The scatter depends on the criteria used to select the model clusters.

ACKNOWLEDGMENTS

AAS acknowledges generous financial support from the Royal Society. We thank T. Shanks for encouraging us to have a closer look at the *K*-band Hubble diagram, and G. Bruzual and S. Charlot for allowing us to use their model results prior to publication. We thank the anonymous referee for useful comments. The version of the Durham semi-analytic models used to produce the predictions in this paper is the result of a collaboration between Shaun Cole, Carlos Frenk, Cedric Lacey and CMB, supported in part by a Particle Physics and Astronomy Research Council rolling grant. This work was carried out under the auspices of EARA, a European Association for Research in Astronomy, and the TMR Network on Galaxy Formation and Evolution funded by the European Commission.

REFERENCES

Abell G. O., 1957, ApJS, 3, 221
Abell G. O., Corwin H. G., Olowin R. P., 1989, ApJS, 70, 1
Aragón-Salamanca A., Ellis R. S., Couch W. J., Carter D., 1993, MNRAS, 262, 764
Aragón-Salamanca A., Ellis R. S., Schwartzenberg J.-M., Bergeron J., 1994, ApJ, 421, 27
Arimoto N., Yoshii Y., 1986, A&A, 164, 260
Barger A. J., Aragón-Salamanca A., Ellis R. S., Couch W. J., Smail I., Sharples R. M., 1996, MNRAS, 279, 1
Barger A. J. et al., 1998, ApJ, in press
Baugh C. M., Cole S., Frenk C. S., 1996a, MNRAS, 283, L15
Baugh C. M., Cole S., Frenk C. S., 1996b, MNRAS, 283, 1361
Baugh C. M., Cole S., Frenk C. S., Lacey C. G., 1998, ApJ in press
Bower R. G., Lucey J. R., Ellis R. S., 1992a, MNRAS, 254, 589
Bower R. G., Lucey J. R., Ellis R. S., 1992b, MNRAS, 254, 601
Bruzual A. G., Charlot S., 1993, ApJ, 405, 538
Burstein D., Heiles C., 1982, AJ, 87, 1165
Cole S., 1991, ApJ, 367, 45
Cole S., Aragón-Salamanca A., Frenk C. S., Navarro J. F., Zepf S. E., 1994, MNRAS, 271, 781
Couch W. J., Ellis R. S., Malin D. F., MacLaren I., 1991, MNRAS, 249, 606
Eke V. R., Cole S., Frenk C. S., 1996, MNRAS, 282, 263
Ellis R. S., Smail I., Dressler A., Oemler Jr. A., Bucher H., Sharples R. M., 1997, ApJ, 483, 582
Fabian A. C., Nulsen P. E. J., Canizares C. R., 1982, MNRAS, 201, 933
Grasdalen G. L., 1980, in Abell G. O., Peebles P. J. E., eds, Proc. IAU Symp. 92, Objects of High Redshift. Reidel, Dordrecht, p. 269
Gunn J. E., Oke J. B., 1975, ApJ, 195, 255
Gunn J. E., Hoessel J. G., Oke J. B., 1986, ApJ, 306, 30
Heyl J. S., Cole S., Frenk C. S., Navarro J. F., 1995, MNRAS, 274, 755
Hoessel J. G., 1980, ApJ, 241, 493
Kauffmann G., 1995, MNRAS, 274, 161
Kauffmann G., 1996, MNRAS, 281, 487
Kauffmann G., Charlot S., 1998, MNRAS, 294, 705
Kauffmann G., White S. D. M., Guiderdoni B., 1993, MNRAS, 264, 201
Kauffmann G., Guiderdoni B., White S. D. M., 1994, MNRAS, 267, 981
Kodama T., Arimoto N., 1997, A&A, 320, 41
Kristian J., Sandage A., Westphal J. A., 1978, ApJ, 221, 383
Lacey C. G., Silk J., 1991, ApJ, 381, 14
Lauer T. R., Postman M., 1992, ApJ, 400, L47
Lebofsky M. J., 1980, in Abell G. O., Peebles P. J. E., eds, Proc. IAU Symp. 92, Objects of High Redshift. Reidel, Dordrecht, p. 257
Lebofsky M. J., Eisenhardt P. R. M., 1986, ApJ, 300, 151
Lilly S. J., 1989a, ApJ, 340, 77
Lilly S. J., 1989b, in Frenk C. S. et al., eds, The Epoch of Galaxy Formation. Kluwer, Dordrecht, p. 63
Lilly S. J., Longair M. S., 1982, MNRAS, 199, 1053
Lilly S. J., Longair M. S., 1984, MNRAS, 211, 833
Lubin L. M., 1996, AJ, 112, 23
Navarro J. F., Frenk C. S., White S. D. M., 1996, ApJ, 462, 563
Oke J. B., Gunn J. E., Hoessel J. G., 1996, AJ, 111, 29
Peach J. V., 1970, ApJ, 159, 753
Peach J. V., 1972, in Evans D. S., ed., Proc. IAU Symp. 44, External Galaxies and Quasi-Stellar Objects. Reidel, Dordrecht, p. 314
Postman M., Lauer T. R., 1995, ApJ, 440, 28
Rakos K. D., Schombert J. M., 1995, ApJ, 439, 47
Sandage A., 1988, ARA&A, 26, 561
Sandage A., Kristian J., Westphal J. A., 1976, ApJ, 205, 688
Scalo J. M., 1986, Fundam. Cosmic Phys., 11, 1
Schneider D. P., Gunn J. E., Hoessel J. G., 1983a, ApJ, 264, 337
Schneider D. P., Gunn J. E., Hoessel J. G., 1983b, ApJ, 268, 476
Smail I., Dressler A., Kneib J.-P., Ellis R. S., Couch W. J., Sharples R. M., Oemler Jr. A., 1996, ApJ, 469, 508
Smail I., Dressler A., Couch W. J., Ellis R. S., Oemler Jr. A., Butcher H., Sharples R. M., 1997, ApJS, 110, 213
Viana P. T. P., Liddle A. R., 1996, MNRAS, 281, 323
White S. D. M., Frenk C. S., 1991, ApJ., 379, 52
White D. A., Fabian A. C., Johnstone R. M., Mushotsky R. F., Arnaud K. A., 1991, MNRAS, 252, 72
White S. D. M., Efstathiou G., Frenk C. S., 1993, MNRAS, 262, 1023

Downloaded from https://academic.oup.com/mnras/article/297/2/427/988365 by guest on 24 April 2024